in the next section.) We have, therefore, the relation

$$\lambda_m/\lambda_s = n_m/n_s \tag{1}$$

The test is started at some chosen value $\theta_m(0)$, with the angular momentum vector vertical and the turntable rotating at the angular velocity λ_m. If the horizontal Cartesian coordinates of the center of mass are designated by $X_0(t)$, $Y_0(t)$, in the laboratory (inertial) frame, it follows that

$$X_0 = -R\cos(\lambda_m t), \qquad Y_0 = -R\sin(\lambda_m t)$$

Hence, the center of mass of the model is accelerated in the horizontal plane by the amounts

$$\ddot{X}_0 = \lambda_m^2 R\cos(\lambda_m t), \qquad \ddot{Y}_0 = \lambda_m^2 R\sin(\lambda_m t)$$

The corresponding force that will appear in a nonrotating reference frame (X',Y',Z') that moves with the center of mass, when combined with the gravitational force, leads to the requirement (Fig. 2)

$$\lambda_m^2 R/g = \tan\theta_m \tag{2}$$

where g is the gravitational acceleration, in order that the vector sum of the forces will be aligned at all times with the model's z axis.

If s is the vertical distance from the center of mass to the horizontal plane of the sensor array (Fig. 1), and r the excursion from the array's null position at $X' = Y' = 0$, then $\tan\theta_m = r/s$. Hence, for the force acting on fluids such as propellants or slag to be a proper follower force and to be proportional to the thrust, we need to require that

$$R = (g/s\lambda_m^2)r \tag{3}$$

A closed-loop electrical network to control R according to this relationship and to control the rotation angle ψ of the turntable is indicated in Fig. 3. Error signals ξ and η are generated by opposing pairs of photoelectric elements when the light beam is not centered on the array (Fig. 1). The quantities $gr/(s\lambda_m^2)$ and $(r+R)\psi$ are generated by the network and control the motors M-2 and M-3 (Fig. 3).

Spacecraft/Model Similarity Relation

The test article is required to be a scale model of the spacecraft, with identical inertia ratios σ and initial nutation angle $\theta(0)$. To simulate the dynamics of fluid sloshing, it is also required that the Froude numbers Fr_m of the model and Fr_s of the spacecraft

$$Fr_m = n_m^2 \ell_m/a_m, \qquad Fr_s = n_s^2 \ell_s/a_s \tag{4}$$

be the same, where a_m and a_s are the acceleration terms parallel to the z axis. For the model, $a_m = g/\cos\theta_m$; for the spacecraft, $a_s = T/m_s$. It follows that the z component n_m of the model's angular velocity must be chosen according to the rule

$$n_m = n_s\sqrt{\ell_s g m_s/\ell_m T\cos\theta(0)} \tag{5}$$

Thus, for instance, for a spacecraft with $n_s = 6.28\ \text{s}^{-1}$ (corresponding to 60 rpm), $\sigma = 0.50$ (hence, a prolate configuration), $T/m_s = 4.0\ g$, $\ell_s/\ell_m = 2.00$, and $\theta(0) = 10.0$ deg, similarity requires $n_m = 4.47\ \text{s}^{-1}$ (corresponding to 42.7 rpm); hence, $\lambda_m = -2.24\ \text{s}^{-1}$. For a test rig design with $s = 20$ cm, it follows that $r = 3.53$ cm, and from Eq. (3), $R = 34.5$ cm.

Conclusion

Contrary to opinions sometimes held, it is possible to design a test rig that is capable of verifying in the laboratory the stability of a space vehicle in the presence of thrust. This is achieved by mounting the scaled or full-scale spacecraft model eccentrically on a rotating platform in such a way that the additional forces introduced in the noninertial reference frame, when added to the laboratory gravity, just provide the lacking (scaled) thrust component.

References

[1]Meyer, R. X., "Convective Instability in Solid Propellant Rocket Motors," *Astrodynamics,* Vol. 54, Advances in the Astronautical Sciences, AAS Paper 83-368, American Astronautical Society, San Diego, CA, 1983.

[2]Flandro, G. A., et al., "Fluid Mechanics of Spinning Rockets," Air Force Rocket Propulsion Lab., Edwards AFB, CA, Rept. TR-86-072, 1986; also, Flandro, G. A., "Interaction of Inertial Waves in a Spinning Propellant Rocket Motor with Spacecraft Motion," Air Force Rocket Propulsion Lab. Rept., 1982.

[3]Mingori, D. L., and Yam, Y., "Nutational Stability of a Spinning Spacecraft with Internal Mass Motion and Axial Thrust," AIAA Paper 86-2271, 1986.

[4]Kaplan, M. H., *Modern Spacecraft Dynamics and Control,* Wiley, New York, 1976, Chap. 2.

Comparison of the Least-Squares Moving-Block Technique with Ibrahim's Method

Ahmed Omar Amrani*
Advanced Rotorcraft Technology, Inc., Mountain View, California 94043

Introduction

MODAL parameters of a given dynamical system can be identified from either the transient time response[1-3] or the forced time response to a control input.[4,5] A new approach for the modal identification from transient time history data is presented here. The method is applied to two test examples to evaluate and compare its performance to the Ibrahim sparse time domain algorithm.

Least-Squares Moving-Block Technique

The theory supporting the least-squares moving-block technique (LSMBT) has already been developed for a single time history[6]; a generalization to any given number of time histories is presented here. Assuming that a number of discretized transient time histories are available from either measurements or computer simulation, the goal is to estimate the modal parameters of the active modes contained in the time history data. Consider a system of p discretized transient signals

$$S_n = \sum_{k=1}^{2m} \eta_k e^{\lambda_k t_n} \qquad t_n = n\Delta t \qquad n = 0,1,2,\ldots \tag{1}$$

$$\lambda_k = -\sigma_k + j2\pi f_k \qquad k = 1,2,3,\ldots,2m \tag{2}$$

$$S_n = \begin{bmatrix} s_{1n} \\ s_{2n} \\ \cdots \\ s_{pn} \end{bmatrix} \qquad \eta = [\eta_1,\eta_2,\ldots,\eta_k,\ldots,\eta_{2m}] \tag{3}$$

Received March 23, 1989; revision received June 16, 1989.

*Aerospace Engineer.

where the matrix η represents the modal matrix associated with the p time signals. The objective is therefore to find the number of active modes m and the corresponding parameters $(\eta_k, \sigma_k f_k)$. The search for the active modes is performed in the frequency domain using the fast Fourier transform (FFT). This is equivalent to searching for the dominant frequencies occurring in the Fourier spectrum. First a frequency resolution Δf is selected. The number of sampled data to run the FFT is

$$Q = 1/(\Delta f \Delta t) \tag{4}$$

Second, the FFT is applied to all p time signals. The collected dominant frequencies are sorted in order to discard the redundant equal frequencies; the number of sorted dominant frequencies gives the number of active modes.

The dampings and modal matrix are estimated using a moving block in the time domain from the known number of active modes and corresponding frequencies. The block length N is selected according to the time data. A natural choice is

$$N = 1/(\min\{f_k\})\Delta t \qquad k = 1,2,3,\ldots, 2m \tag{5}$$

Several block lengths can be selected; however, when more than one time signal is considered, a relatively larger block length yields better results, especially in the presence of noise.

Consider the first block. The following matrices are defined

$$S = [S_0 S_1 \cdots S_{N-1}] \tag{6}$$

$$Z = \{e^{j2\pi f_k n\Delta t}\} \qquad k = 1,2,3,\ldots, 2m \qquad n = 0,\ldots, N-1 \tag{7}$$

A pseudomodal matrix Ψ is computed as a solution to the least-squares problem formulated by the following equation

$$S = \Psi Z \tag{8}$$

The least-squares solution is

$$\Psi = SZ^T(ZZ^T)^{-1} \tag{9}$$

The calculation of the pseudomodal matrix Ψ is repeated for l subsequent blocks, of the same size N, moving with step size K_B along the time axis. The collected results are

$$\Psi^{(1)}, \Psi^{(2)}, \ldots, \Psi^{(l)} \tag{10}$$

Matrices U and V are defined as the partial sums

$$U = \Psi^{(1)} + \Psi^{(2)} + \cdots + \Psi^{(l-1)} \tag{11}$$

$$V = \Psi^{(2)} + \Psi^{(3)} + \cdots + \Psi^{(l)} \tag{12}$$

The damping estimates averaged over all blocks are

$$\sigma_k = \frac{\log\|u_k\| - \log\|v_k\|}{K_B \Delta t} \qquad k = 1,2,3,\ldots, 2m \tag{13}$$

where K_B is the moving-block step size.

The modal matrix is estimated from the pseudomodal matrix using the damping estimates and the block time length T. The pseudomodal matrix is approximated as an average over one block period of the modal matrix multiplied by the exponential decay of all modes. An algebraic expression for the modal matrix is consequently deduced from the approximation just mentioned:

$$\eta = \Psi \text{diag}\left(\left\{\frac{\sigma_k T}{1 - e^{-\sigma_k T}}\right\}\right) \qquad k = 1,2,3,\ldots, 2m \tag{14}$$

with

$$T = N\Delta t \tag{15}$$

Test Case Application

This test case evaluates the performance of the LSMBT using the eigenvectors of a dynamical system written in first-order form. This is of particular interest because time history data generated by computer simulations are often available in first-order form. The eigenvectors are generated from a mass-spring-damper system with five degrees of freedom and with unit mass, unit stiffness, and a value of 0.2 for the damping coefficient. The modal frequencies and damping ratios, which assume the value of 2%, are taken from Ref. 2. Table 1 indicates the modal frequencies. These modal parameters are consequently used to generate a number of 10 time histories.

The search for the dominant frequencies is depicted in Table 1 for the first five time signals. The remaining five time signals exhibit identical results. The distribution of the dominant frequencies among the five time signals is described by an "X" for every occurrence of any of the modal frequencies. The first two time signals contain all modal frequencies; Fig. 1 illustrates the Fourier spectrum of these two time signals. The time increment, the frequency resolution, and the length of the FFT sequence for this example are

$$\Delta t = 0.0157 \text{ s}, \qquad \Delta f = 0.5 \text{ Hz}, \qquad Q = 128$$

The influence of the number of blocks on the damping ratios is presented in Table 2; the estimates obtained using only two blocks closely approach the exact values. The block length computed from Eq. (4) is $N = 50$, and the block step size is $K_B = 50$.

Table 1 Distribution of dominant frequencies

	Numbered time signals				
Frequency, Hz	1	2	3	4	5
10	X	X	X	X	X
12	X	X	X	--	--
15	X	X	X	X	X
20	X	X	--	X	X
21	X	X	X	--	--

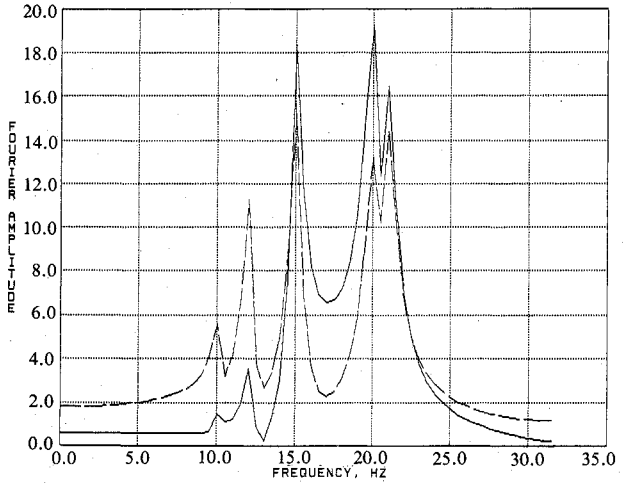

Fig. 1 Occurrence of dominant frequencies in the Fourier spectrum for time signals 1 and 2.

Table 2 Influence of block number on the damping ratio, %

	Number of moving blocks			
Mode no.	2	3	4	5
1	1.998	2.007	2.012	2.013
2	1.854	2.107	2.150	2.027
3	1.988	2.000	2.001	1.998
4	1.973	1.987	2.004	2.015
5	1.944	1.932	1.948	1.969

Table 3 Influence of noise on damping ratio, %

Mode no.	Percent noise-to-signal ratio			
	0	10	30	50
1	2.040	2.037	2.059	1.974
2	2.054	2.036	2.086	1.949
3	2.004	2.009	2.073	2.110
4	1.989	2.013	2.197	1.759
5	2.016	2.005	1.941	2.150

Table 4 Comparison of results between the sparse time domain algorithm and the least-squares moving-block technique

Mode no.	Frequency, Hz			Damping ratio, %		
		30% N/S ratio			30% N/S ratio	
	Exact	STD	LSMBT	Exact	STD	LSMBT
1	10.00	9.99	10.00	2.00	2.11	2.06
2	12.00	11.99	12.00	2.00	2.05	2.07
3	15.00	15.00	15.00	2.00	2.03	2.07
4	20.00	20.01	20.00	2.00	2.02	2.20
5	21.00	21.03	21.00	2.00	1.99	1.94

To improve the accuracy of the results, scaling factors for the time history data may be used. In particular, scaling factors can be selected in such a way as to force the peak-to-peak amplitude of the first block to be the same for all time signals.

Comparison to the Ibrahim Sparse Time Domain Algorithm

The LSMBT is applied to the numerical test solved by the sparse time domain (STD) algorithm in Ref. 2 using the same modal frequencies, damping ratios, and eigenvectors. The selected time increment, frequency resolution, block length, block step size, and number of blocks are

$$\Delta t = 0.004 \text{ s}, \quad \Delta f = 0.5 \text{ Hz}, \quad N = 100, \quad K_B = 100, \quad l = 3$$

Random numbers with a uniform distribution are added to the time history data for a given noise-to-signal ratio. The influence of noise on the damping ratio estimates is shown in Table 3. Good estimates for the damping ratios are retained up to a high 50% N/S ratio. The effect of noise is governed by the number of sampled data $p \times N \times l$. As statistically expected, a large number of data yield better accuracy. In this application $p = 10$, thus, $p \times N \times l = 3 \times 10^3$; the size of the matrix holding time data used by the STD is $210 \times 40 = 8.4 \times 10^3$. This is about three times as many data for the STD as compared to the LSMBT. However, by increasing the problem size to reduce the noise effect, computer storage and numerical errors also increase.

The comparison of results between the LSMBT and the STD is given in Table 4. The modal frequencies are recovered exactly in the case of the LSMBT. More important, the damping ratio estimates are comparable for the two methods even though the LSMBT uses lesser data.

Conclusions

The least-squares moving-block technique (LSMBT) has been shown to yield comparable results to the Ibrahim sparse time domain algorithm. However, the implementation of the LSMBT has the following advantages:

1) A relatively large number of time signals are not required. In fact, the method can be applied starting from a single time signal. This is of interest because experimental data are not always available at a large number of recording stations.

2) There is no need to postprocess the results to separate computational and physical modes.

3) There is no need for an initial guess of system order.

4) Control over the accuracy is achieved by increasing or decreasing the number of blocks.

5) Computer storage and CPU time are reduced.

The implementation advantages and results of this new method demonstrate its strong capability as a tool for modal identification.

References

[1]Hammond, C. E., and Dogget, R. V., Jr., "Determination of Subcritical Damping by Moving-Block/Randomdec Applications," NASA SP-415, Oct. 1975.

[2]Ibrahim, S. R., "An Approach for Reducing Computational Requirements in Modal Identification," *AIAA Journal*, Vol. 24, No. 10, 1986, pp. 1725–1727.

[3]Kauffman, R. R., "Application of the Ibrahim Time Domain Algorithm to Spacecraft Transient Responses," AIAA Paper 84-0946, May 1984.

[4]Juang, J.-N., and Pappa, R. S., "An Eigensystem Realization Algorithm for Modal Parameter Identification and Model Reduction," *Journal of Guidance, Control, and Dynamics*, Vol. 8, No. 5, 1985, pp. 620–627.

[5]Ljung, L., and Soderstrom, T., *Theory and Practice of Recursive Identification*, MIT Press, Cambridge, MA, 1983.

[6]Omar Amrani, A., and Du Val, R., "Parameter Identification of Aeroelastic Modes of Rotary Wings from Transient Time Histories," *Journal of Guidance, Control, and Dynamics* (to be published).

Contribution of Zonal Harmonics to Gravitational Moment

Carlos M. Roithmayr*
NASA Johnson Space Center, Houston, Texas 77058

Introduction

THE gravitational moment about the mass center of a body in orbit about a celestial body has an important effect on the orientation of the orbiting body. The more misshapen the celestial body, and the less uniform its mass distribution, the more involved is the calculation of the gravitational moment (and force) it exerts. Situations in which it might be important to calculate accurately the gravitational moment include the design of spacecraft for expeditions to asteroids, comets, and the moons of Mars.

In Ref. 1, a method for obtaining a vector-dyadic expression for the moment exerted about a small body's mass center by an oblate spheroid was set forth. The derivation of that expression made use of a gravitational potential written in terms of the zonal harmonic of the second degree. When gravitational potentials containing zonal harmonics of degree 2 or greater are considered, each zonal harmonic makes a contribution to the gravitational moment.

What follows is a vector-dyadic expression for the contribution of a zonal harmonic of degree n to the gravitational moment, produced by a body, about the mass center of a small body. As is the case with all vector-dyadic expressions, this result is basis-independent—that is, the vectors and dyadics can be expressed in any convenient vector basis.

The equation that follows is recursive: The contribution to the gravitational moment from the zonal harmonic of degree

Received April 6, 1989; revision received June 21, 1989.

*Aerospace Engineer, Guidance and Navigation Branch.